THE STATIC AND QUASI-DYNAMIC RESPONSE OF GRAPHENE SENSORS: THE IMPACTS OF SURFACE DEFECTS

by

Aaron Lowenberger

A Thesis
Submitted to the
Graduate Faculty
of
George Mason University
in Partial Fulfillment of
The Requirements for the Degree
of
Master of Science
Electrical Engineering

Committee:

_____	Dr. Qiliang Li, Thesis Director
_____	Dr. Dimitris Ioannou, Committee Member
_____	Dr. Patrick Vora, Committee Member
_____	Dr. Monson H. Hayes, Department Chair
_____	Dr. Kenneth S. Ball, Dean, Volgenau School of Engineering

Date:_____ Fall Semester 2017
George Mason University
Fairfax, VA

The Static and Quasi-Dynamic Response of Graphene Sensors: The Impacts of Surface Defects

A Thesis submitted in partial fulfillment of the requirements for the degree of Master of Science at George Mason University

by

Aaron Lowenberger
Bachelor of Science
Boston University, 2002

Director: Qiliang Li, Professor
Department of Electrical Engineering

Fall Semester 2017
George Mason University
Fairfax, VA

DEDICATION

This is dedicated to my loving and supportive wife, Amanda, and my wonderful son Nathan.

ACKNOWLEDGEMENTS

I would like to thank the many friends, relatives, and supporters who have made this happen. I would also like to thank Dr. Qiliang Li for his patience, assistance, and guidance.

TABLE OF CONTENTS

LIST OF TABLES

LIST OF FIGURES

ABSTRACT

THE STATIC AND QUASI-DYNAMIC RESPONSE OF GRAPHENE SENSORS: THE IMPACTS OF SURFACE DEFECTS

Aaron Lowenberger, M.S.

George Mason University, 2017

Thesis Director: Dr. Qiliang Li

Chemical sensors are widely used in many technologies, with applications in medicine, industrial process monitoring, automotive and aerospace, military, and environmental protection. Due to the excellent electronic properties and unique two-dimensional (2D) structure, graphene has shown great promise as a highly sensitive, low noise sensor material. This research was to explore the static and dynamic response of graphene sensors upon exposure to different chemical vapors. Different graphene sensor configurations, including pristine graphene and graphene with four typical types of surface defects, were modeled in the presence and absence of five different chemicals. First-principle simulations were performed to study the electrostatic response of the different sensor configurations. The results were analyzed and compared with previously published experimental data, revealing the dominating defects present in the experimental sensors. In addition, the dynamic response of graphene sensors and the molecule-graphene interaction mechanism has been investigated by progressively changing the

distance between the sensor and the vapor molecules. This study is very important for understanding the reaction mechanism between a 2D surface and chemical molecules, leading to high-performance chemical sensors.

CHAPTER 1 – WHY GRAPHENE SENSORS?

1.1 Sensor Market Trends

Chemical sensors are widely used in many fields today. For example they find applications in the pharmaceuticals industry, automotive industry, chemical processing, environmental monitoring, industrial safety, and healthcare. As technology advances, sensors are used in ever more devices and the sensor market grows accordingly. The global market for sensors is predicted to reach US $241 billion in 2022. Major drivers of this trend include the growing adoption of the Internet of Things (IoT), increasing demand for wearables, and the increasing usage of many kinds of sensors in smartphones.[1]

The chemical sensor market will be a large part of this growth in the sensor market. The global chemical sensor market is projected to reach US $31.2 by 2020. Biosensors, which find applications in wearables and IoT, are a large driver of this growth in the chemical sensors market.[2] Furthermore, the environmental gas sensor market is projected to reach US $3 billion by 2027.[3]

These projections show that there are great opportunities in developing and understanding novel sensor materials and devices. To that end, the impetus for this work is to explore the use of graphene as a sensor material, and specifically the role that surface defects in the detection of chemicals by graphene sensors.

1.2 Sensor Materials and Designs

Due to the importance of chemical sensing in such a wide variety of fields, chemical sensors come in many forms and are made from a variety of materials. In general, sensors work by exploiting some physical phenomenon which can be converted into an electrical signal. What follows is a brief summary of some common sensor materials and devices.

Metal-oxide semiconductor sensors operate based on a change in electrical conductivity when the sensor surface comes into contact with a gas. Generally, Metal Oxide Semiconductor sensors come in either type n sensors or type p sensors. Type n sensors, such as ZnO and SnO_2, change resistance in the presence of a reducing gas, while type p sensors, such as NiO and CoO, change resistance in the presence of oxidizing gases.[4,5]

Surface acoustic wave (SAW) sensors comprise a sensing layer and a transducer, generally a piezoelectric substrate. Any adsorption of gases on the sensing layer causes some frequency shift from a reference frequency in the transducer, which can then be measured in order to detect the presence of gases.[6]

Carbon based materials have also been shown to have applications as chemical sensors. Carbon black composites with polymers have been shown to make chemical sensitive resistors, with a broad response to a variety of chemicals. Similar to other chemiresistor type sensors, the change in conductance of the sensor is monitored in order to detect the presence of chemicals being sensed.[7,8]

Carbon nanotube based sensors have shown that carbon-based nanostructures can be used as materials for sensor devices. These sensors operate by monitoring the conductivity of single-walled carbon nanotubes (SWNTs). The electrical resistance of semiconducting SWNTs is seen to change when the SWNTs are exposed to gases such as NO_2 and NH_3. They have shown linear responses as well as detection thresholds down to parts-per-billion.[9,10]

Graphene is yet another carbon based material that has been used in chemical sensing applications. Graphene sensors generally work as chemiresistive sensors, similar to many of the previously discussed sensor types, where a change in resistance of the sensor is monitored.

1.3 Graphene Sensors

Graphene has several properties that make it an advantageous material from which to construct sensors. First, graphene is a two-dimensional hexagonal lattice of carbon atoms. This two-dimensional structure means that graphene has a very high surface area-to-weight ratio. In fact, every atom in a single layer graphene sensor is a surface atom, which means that every atom in the sensor is sensitive to the presence of molecules in the sensor environment. This makes for sensors that show appreciable responses down to very low concentrations of chemicals in the environment.

Graphene also shows a very high conductivity even with low carrier densities. The conductance of graphene monolayers is larger than any metal at room temperature. This very high conductance leads to very low levels of thermal noise. This very low noise floor is important for increasing the sensitivity of sensors to even lower concentrations.

Graphene interacts with materials in a variety of ways, including weak van der Walls forces and strong covalent bonds. These different interactions allow for graphene-based sensors to interact with a wide range of different chemicals. Furthermore, the different types of interactions result in sensors that are not only sensitive to different chemicals, but show discrimination amongst them.[11,12]

Four-probe measurements are relatively easy to make on a single graphene device with low-resistance ohmic contacts. This improves the performance of graphene sensors by even further decreasing the influence of noise and improving the accuracy of measurements.

In addition to its superior electronic properties, graphene also has exceptional mechanical properties that make it an attractive material. Graphene is a very light, durable, and flexible material. All of these properties lend themselves to producing sensors that are viable in wearable applications, which require sensors that are able to withstand various stresses without weighing down the person wearing the sensor.

Many research groups have performed investigations into graphene gas sensors. Schedin et al. created graphene gas sensors prepared by micromechanical cleavage and measured changes in resistivity when the prepared sensors were in the presence of gases such as NO_2, NH_3, H_2O, and CO as compared to when the sensors were not in the presence of these gases. They noted that the change in resistivity was dependent on the sensed gas, with some gases causing a positive change and others causing a negative change. Importantly, they also found that the sensors were able to detect even a single molecule of the sensed gas at room temperature.[13]

Leenaerts et al. performed first-principles calculations studying the interactions between pristine graphene and different gas molecules using first-principles calculations using density functional theory (DFT) calculations. They showed that sensor response was nearly independent of the adsorption site but strongly dependent on the orientation of the gas molecule with respect to the graphene surface.[14]

Ko et al. demonstrated that mechanically exfoliated graphene layers on a SiO_2/Si substrate to could be used to create gas sensors with fast response, good reversibility, selectivity, and high sensitivity. They report a sensitivity of 9% when the sensors are exposed to 100ppm NO_2 at room temperature.[15]

Chen et al. synthesized highly sensitive two-terminal graphene sensors using chemical vapor deposition. Sensor response was measured upon exposure to a number of different gases including NO, NO_2, NH_3, N_2O, O_2, SO_2, CO_2, and H_2O. They reported detection limits down to 158 ppq (parts per quintillion) for exposure to NO. They also measured the Raman spectrum at a number of locations on their sensors and measured only weak D-band and D'-band peaks, indicating that the sensors had only a small number of defects.[16]

Nallon et al. exposed graphene produced from chemical vapor deposition (CVD) in order to explore improving the selectivity of graphene gas sensors. The sensors were exposed to a chemically diverse set of compounds including ketones, ethers, hydrocarbons, organosulfurs, and acids, and the change in resistance was measured over time. Principle component analysis was applied to the measured data in order to classify the measured gases with a high level of prediction accuracy. A second experiment was

performed with a set of chemically similar compounds which also resulted in a high level of prediction accuracy.[17]

Seekaew et al. reported a highly sensitive room temperature gas sensor based on bilayer graphene. Their sensor was fabricated by transferring chemical vapor-deposited graphene onto nickel electrodes. They reported that these bilayer graphene sensors showed significantly higher response to NO_2 as compared to monolayer, three layer, and four layer sensors. Interestingly, the Raman spectra reported by Seekaew et al. show a significant D-band, indicating disorder in their graphene sheets, and therefore, the presence of defects in the graphene lattice.[18]

1.4 Role of Defects in Graphene Sensors

While graphene has superior electronic qualities, it is somewhat surprising that it has proven to show such promise as a gas sensor. Graphene is a zero-bandgap material that behaves as a semi-metal. Semimetals are not expected to be sensitive to electric fields. For example, graphene does not show a very large field-effect behavior. Top-gated transistors fabricated from a single layer of graphene have been developed but they generally suffer from poor on/off ratios due to the absence of a bandgap in graphene.[19]

Due to its two-dimensional structure, it is expected that graphene sensors should be very sensitive to surface defects. The presence of even a single surface defect should have an effect on the response of a graphene sensor because every surface atom is available to be involved in both sensing and conduction. Results reported previously in the literature tend to support the hypothesis that surface defects play an important role in graphene sensors.

While investigating the electronic response of single-walled carbon nanotubes (SWNT) to trace levels of chemical vapors, Robinson et al. found that surface defects had a large impact on the sensing behavior of the SWNT. They report that the electronic response to chemical vapors is in fact dominated by adsorption at the defect sites. They reported that the defect sites act as low-energy adsorption sites for the vapors, and that the sensitivity of the SWNT sensors can be increased significantly with the introduction of defects.[20]

Salehi-Khojin et al. showed that linear defects enhance the chemical sensitivity in graphene based sensors. They reported that graphene sensors made with linear defects were found to have a greater response than graphene with point defects or pristine graphene.[21]

Dan et al. noted that conventional nanolithography, when used to pattern graphene to manufacture sensors, leaves a residue on the graphene, but that the effect of this residue had not previously been investigated. They found that the resist residue chemically dopes the graphene and acts as an absorbent layer that enhances graphene sensor response. They reported that graphene sensors from which the residue had been cleaned showed a significantly smaller response than graphene sensors on which the residue was maintained.[22]

First-principle simulations have shown that nitrogen-vacancy zigzag graphene nanoribbons are better gas sensors than pristine zigzag graphene nanoribbons, and that unique resonant peaks of transmission created with adsorption of different gases can be used to detect which specific gas has been adsorbed.[23] Other first-principle studies have

shown that surface defects can be used to improve the sensitivity of graphene gas sensors when sensing gases such as SO_2, CO, NO, NO_2, and NH_3.[24,25]

Yang et al. performed first-principles calculations exploring methane adsorption on graphene sensors. They reported that the adsorption energy of methane on graphene at the site of vacancy defects in a graphene sensor is lower than the adsorption energy of pristine graphene.[26]

It is clear that the electrical properties and sensing behavior of graphene is greatly affected by surface defects. Understanding the effects of surface defects on graphene gas sensors is critical to designing sensitive and selective sensors.

1.5 Focus of this Work

In this thesis, first-principles calculations were performed to study the effect of four different surface defects on the sensing behavior of graphene gas sensors. The results of these simulations show that pristine graphene is significantly less sensitive to the presence of environmental gases than any of the defective graphene sensors that were studied. Additionally, the results demonstrate that each different surface defect alters the sensing response of the sensor differently for each of the different studied gases, indicating that it may be possible to engineer graphene to respond in such a way as to generate the response that is desired for a specific application. The orientation of the adsorbed gas molecule was found to have a large impact on the sensor response. Based on a comparison with previously reported experimental data, the orientation of several different gas molecules with respect to the graphene sensor surface was discovered.

Additionally, the surface defects that dominated the response of the previously reported sensors was determined.

CHAPTER 2 – EXPERIMENTAL PROCEDURES

2.1 Simulation of IV Curves

In this study, first-principle calculations were carried out using the QuantumWise Virtual Nanolab Atomistix Toolkit (ATK) package.[27] First, small graphene nanosheets consisting of 48 carbon atoms with a chiral vector of n=2, m=2 were modeled. This size was chosen because it was computationally relatively inexpensive even when using density functional theory (DFT) for relaxing molecular geometries. Then, these modeled nanosheets were modified with four different surface defects: a vacancy defect, a hydrogen defect, a hydroxyl defect, and an oxygen defect. The structures were then relaxed to optimize force to .05eV/Å and stress to 0.1GPa. To model graphene sensors being exposed to each of the five different gases that were studied (ammonia, toluene, hexane, tetrahydrofuran, and acetone), another relaxation was performed with each of the different surfaces in proximity with each of the different molecules. This relaxation was performed with the same parameters. Finally, to model an actual graphene sensor, each optimized structure including a molecule of analyte was fused with two larger graphene nanosheets. The sizes of these sheets were chosen to be approximately 3nm x 3nm and 4nm x 4nm. The 3nm x 3nm size was chosen to approximate exposure to a given gas at standard temperature and pressure. The 4nm x 4nm size was chosen to give another data point with a slightly lower concentration and defect density for comparison. Each sensor

was modeled as having two electrodes of approximately 9Å length each. A bias voltage was then applied across the sensor and current through the sensor was measured. Thus, each sensor is comprised of three regions: a left electrode, a central region which is either pristine graphene or graphene with a single surface defect and which is exposed to a molecule of gas, and a right electrode region. Electrode regions are treated semi-infinitely. Their properties are computed by solving for bulk material. An I-V curve was then calculated for each of the 60 different sensor configurations (3nm x 3nm and 4nm x 4nm, 4 different surface defects and pristine, and 5 different analytes and no analyte). The I-V curve calculation was performed with the semi-empirical Extended Hückel Theory (EHT) method instead of the DFT method. The EHT method was chosen because the DFT model is computationally prohibitive for systems having more than about 200 atoms and because the EHT seems to be a good tradeoff by capturing most of the electronic and atomic structure effects present in more rigorous methods while remaining computationally inexpensive.[28] The I-V curve calculation was performed using a Monkhorst–Pack k-grid mesh with periodic boundary conditions only in the direction transverse to the flow of current. Bias points of 0.01V and 0.1V were selected to keep the electric field within the graphene sensor below 106V/cm.

2.2 Comparison with Experimental Data

After collecting the I-V curve data, the data was then compared to results reported by Schedin et al.[13] for ammonia and those reported by Nallon et al.[17] for toluene, tetrahydrofuran, hexane, and acetone. The results reported by these groups are summarized in Table 1. Based on this comparison, worked to discover what types of

defects may have dominated the behavior of the experimentally reported sensors. Since it would be nearly impossible for the simulated results to show identical changes in resistance as those that were experimentally reported, the focus was on finding a combination of defects that would qualitatively match the experimentally reported results. This was done by finding a linear combination of simulated defects to find a surface defect configuration that would result in a positive or negative change in resistance that matches the reported result for each of the five different gases.

Table 1 - Summary of %ΔR results reported by Schedin et al.[13] and Nallon et al.[17]

Ammonia	Toluene	Tetrahydrofuran	Hexane	Acetone
4.00%	-0.31%	2.52%	-0.25%	1.00%

2.3 Quasi-Dynamic Simulation

In this research, an attempt was also made to model the dynamic interactions of graphene gas sensors with gas molecules. There are many variables that affect the dynamic response of sensors in real-world experiments that are very difficult to model with first-principles simulation. Instead of trying to account for each of the different parameters that may affect this response, a parameter was proposed that is referred to as "modeled average distance" in an attempt to capture dynamic behavior. The modeled average distance is modeled as the height of a molecule of gas from a reference point, where the reference point is the optimized position of the gas found during the geometric relaxation performed earlier. Thus, a modeled average distance of 0Å would be modeled as a molecule of gas at the height found during relaxation of the geometry of the sensor when exposed to the gas, and a modeled average distance of 1Å would be modeled as a

molecule of gas 1Å above the optimized height, and so on. Figure 1 shows a model of a sensor with an acetone molecule at each of the simulated modeled average distances. IV curves were simulated for each different gas molecule at multiple different modeled average distances (1Å, 2Å, and 3Å above the optimized height). The resistance derived from these IV curves was subtracted from the resistance shown by a sensor in the absence of any gas molecules to find a %ΔR. A response curve was generated by fitting these results to a curve of the form $\%\Delta R = A(1-e^{kt})$, and the curve was compared to experimental results from the literature.

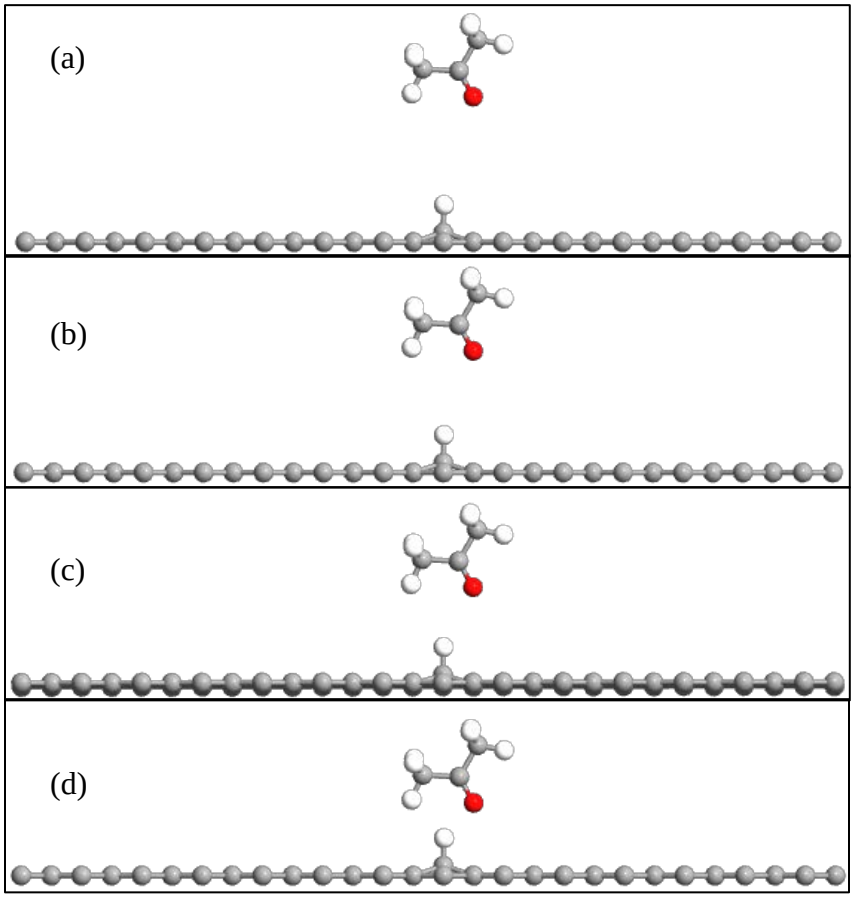

Figure 1 - Graphene sensor with a hydrogen surface defect with a molecule of acetone at a modeled average distance of (a) 3Å (b) 2Å (c) 1Å and (d) 0Å.

CHAPTER 3 – RESULTS AND DISCUSSION

In this section, the results of the first-principles simulations are discussed. First, the results showing the key role played by surface defects on the behavior of graphene gas sensors is detailed. Then the effect of the orientation of a sensed gas molecule on the response of a graphene gas sensor with a given surface is explored. The discussion specifically focuses on the effect of the orientation of acetone and hexane on the response of sensors with a hydrogen surface defect. Finally, a discussion of the comparison of the simulated results to those experimentally reported by Schedin et al. and Nallon et al. follows. Based on this comparison, the surface defect that dominated the response of the experimentally reported results is determined.

3.1 Key Role of Surface Defects in the Response of Graphene Gas Sensors

In the performed simulations, the effects of four different surface defects on the behavior of graphene sensors was studied, in addition to the behavior of pristine graphene sensors. The studied defects included a vacancy defect, in which one carbon atom has been removed from the hexagonal graphene lattice; a hydrogen defect, in which a single hydrogen atom has been bonded to the graphene sensor surface; an oxygen defect, in which a single oxygen atom has been bonded to the graphene sensor surface; and a hydroxyl defect, in which a singly hydroxyl group (OH) has been bonded to the graphene

sensor surface. Figure 2 shows a top view and a side view of each of these defects, as well as a top view and a side view of a pristine graphene sheet.

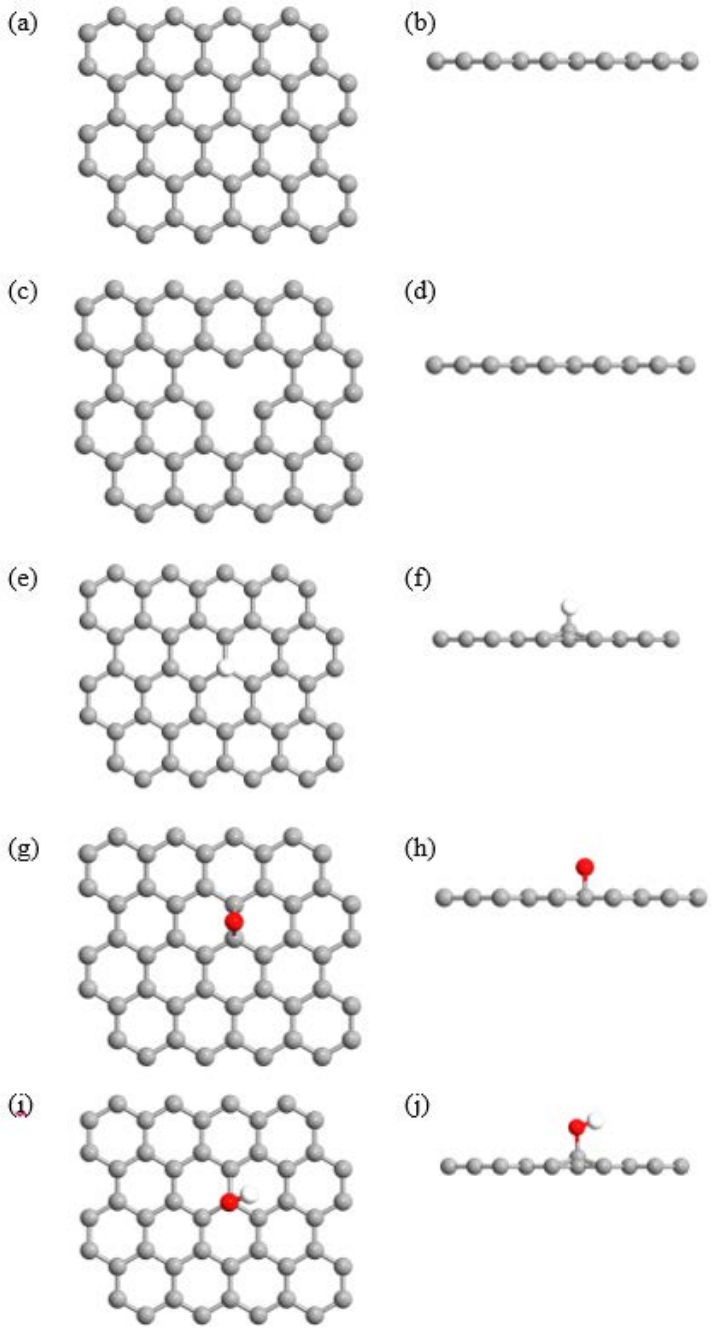

Figure 2 - Top (a) and side (b) view of pristine graphene. Top (c) and side (d) view of graphene with a vacancy surface defect. Top (e) and side (f) view of graphene with a hydrogen surface defect. Top (g) and side (h) view of graphene with an oxygen surface defect. Top (i) and side (j) view of graphene with a hydroxyl surface defect.

Figures 3-7 show the simulated band structures of each different sensor configuration. Figure 3 is the simulated band structure of a pristine graphene sensor. The characteristic zero-bandgap at the K point of graphene can clearly be seen here between the Γ point (identified as G) and Z point. The linear shape of the band edges at this point is also clear in this plot of the band structure. Figures 4 and 5 show the simulated band structure for sensors with a vacancy surface defect and an oxygen surface defect, respectively. Both of these band structures show that a bandgap has opened up as there is no longer a point near the Fermi level where the band edges meet. Interestingly, both of these band structures show a nearly flat band in the vicinity of the Fermi level. Figure 6 shows the simulated band structure for a sensor with an oxygen surface defect. This band structure shows that this particular sensor configuration also appears to have a zero-bandgap. This can be explained as due to the fact that the sensor in this configuration contains no vacancies or sp3 bonded carbon atoms, as can be seen in Figure 2. Finally, Figure 7 shows the simulated band structure for a sensor with a hydroxyl surface defect. This band structure shows neither the zero-bandgap near the K point or a nearly flat band as is seen in the other band structures.

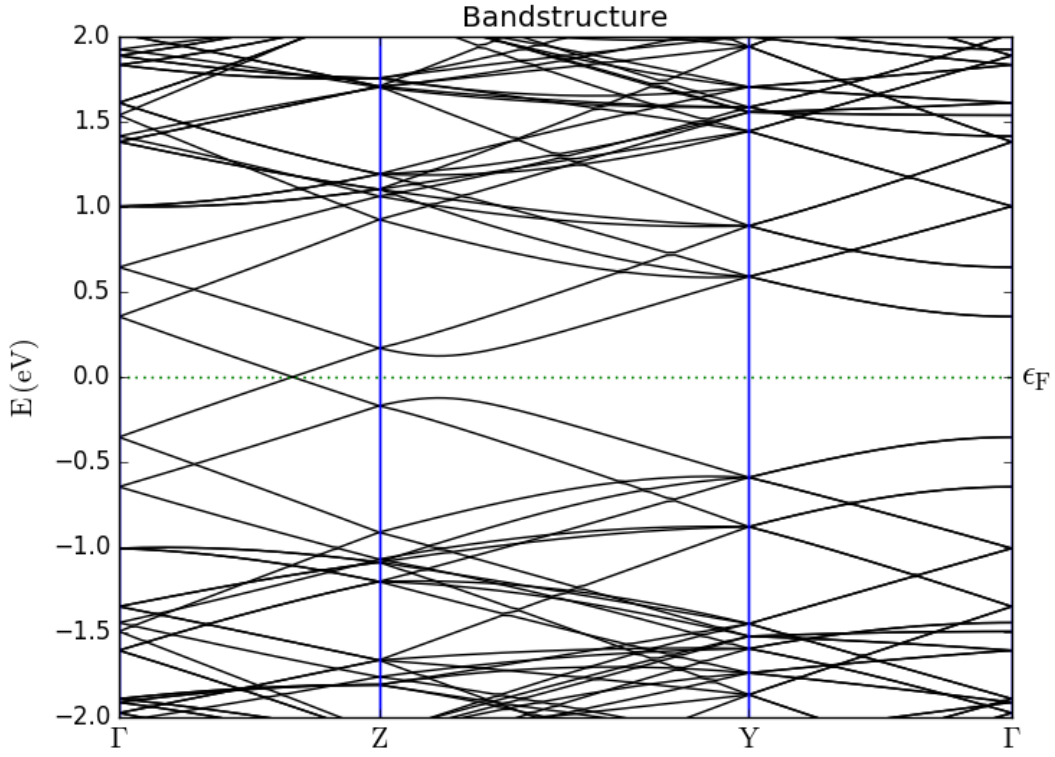

Figure 3 - Band structure of a pristine graphene sensor.

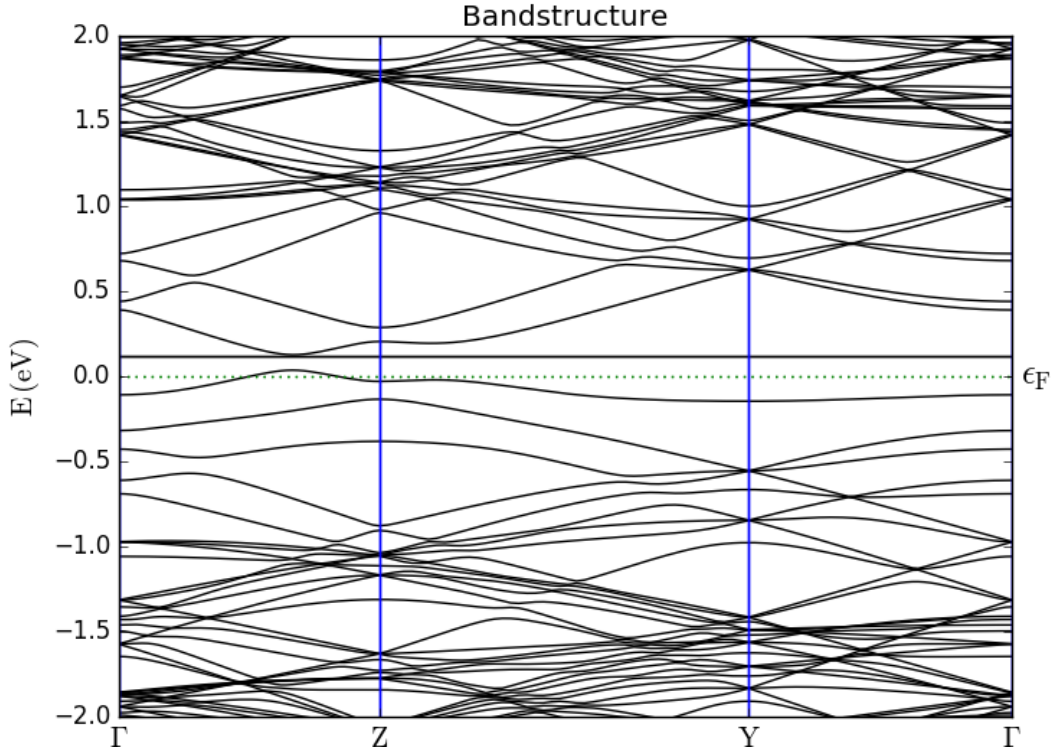

Figure 4 - Band structure of a graphene sensor with a vacancy defect surface configuration.

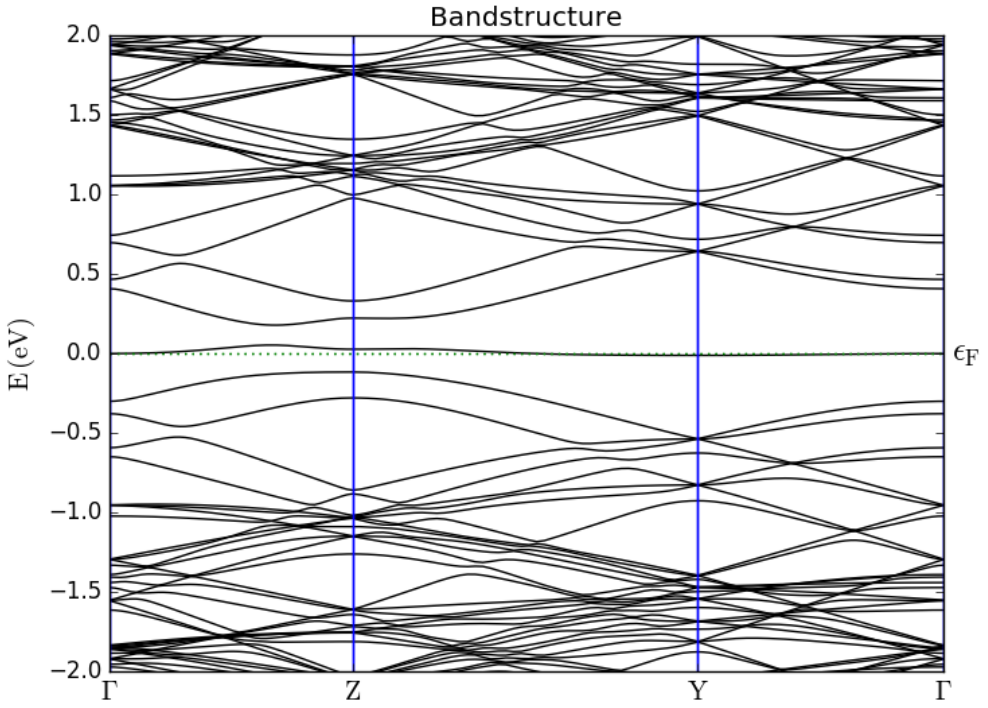

Figure 5 - Band structure of a graphene sensor with a hydrogen defect surface configuration.

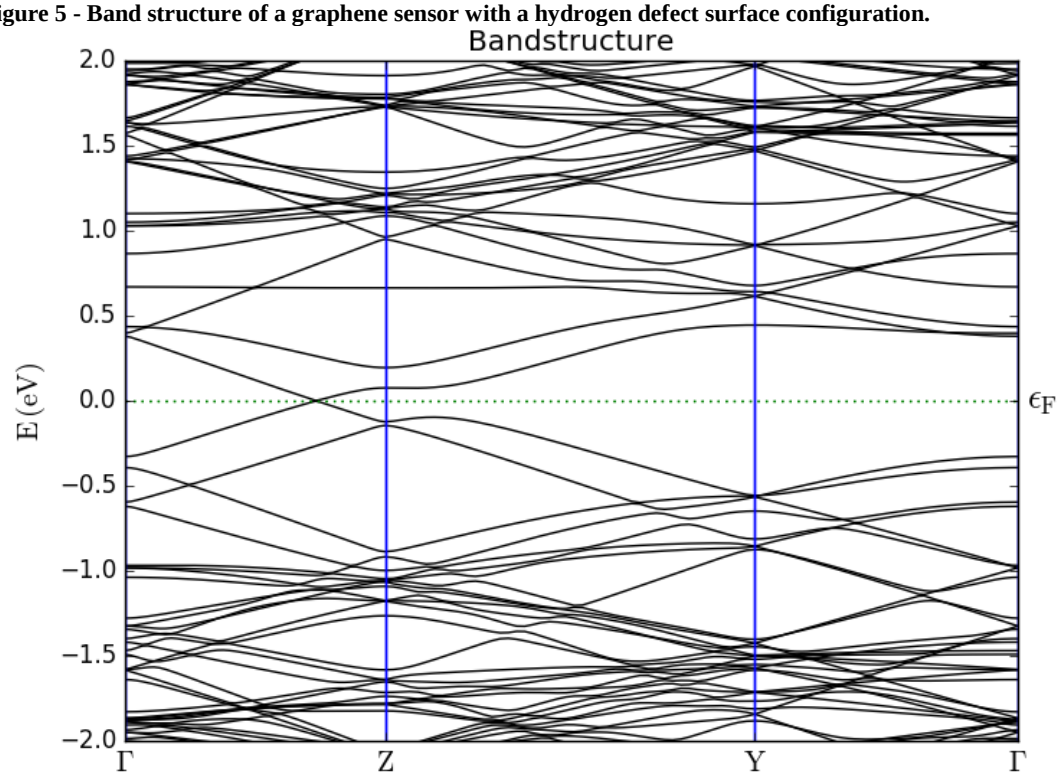

Figure 6 - Band structure of a graphene sensor with an oxygen defect surface configuration.

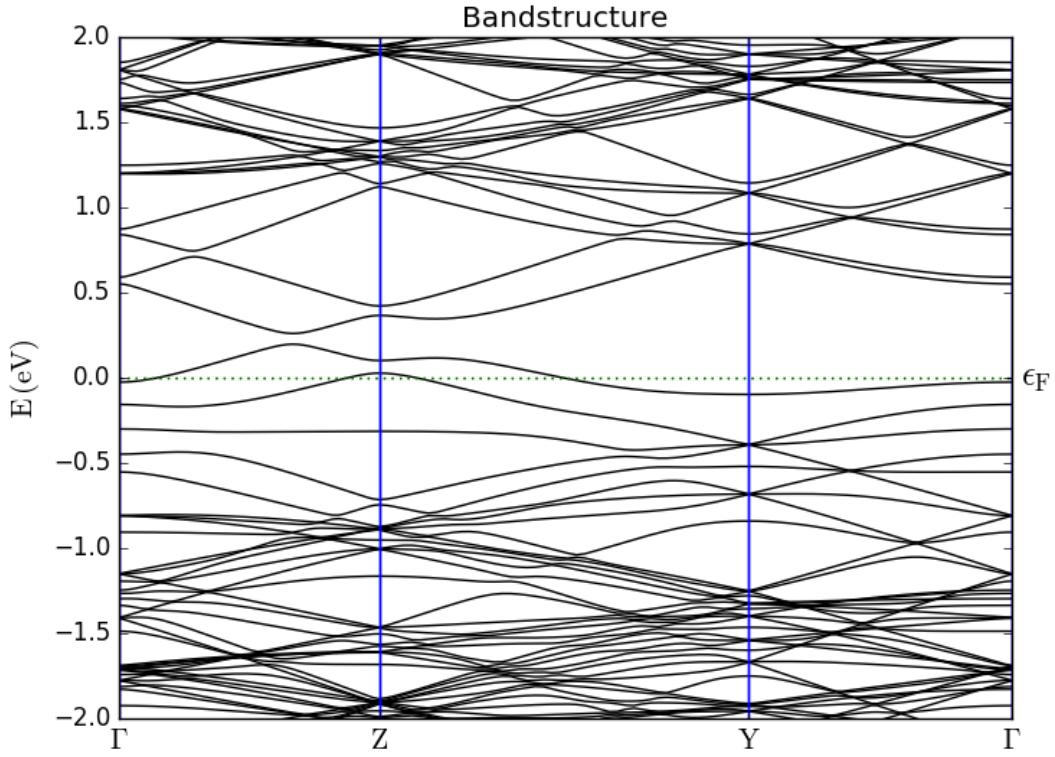

Figure 7 - Band structure of a graphene sensor with a hydroxyl defect surface configuration.

Figures 8-12 show the simulated resistance of each sensor when biased at 0.01V and 0.1V for each of the five different surface configurations (pristine graphene, vacancy surface defect, hydrogen surface defect, oxygen surface defect, and hydroxyl surface defect). The graphs show the response of the sensors when no gas is present as well as when the sensors are exposed to ammonia, toluene, tetrahydrofuran, hexane, and acetone. Table 2 and Table 3 organize this data slightly differently by showing the percent change in resistance of each of the 3nm x 3nm and 4nm x 4nm sensors when exposed to a gas compared to the sensor in a vacuum.

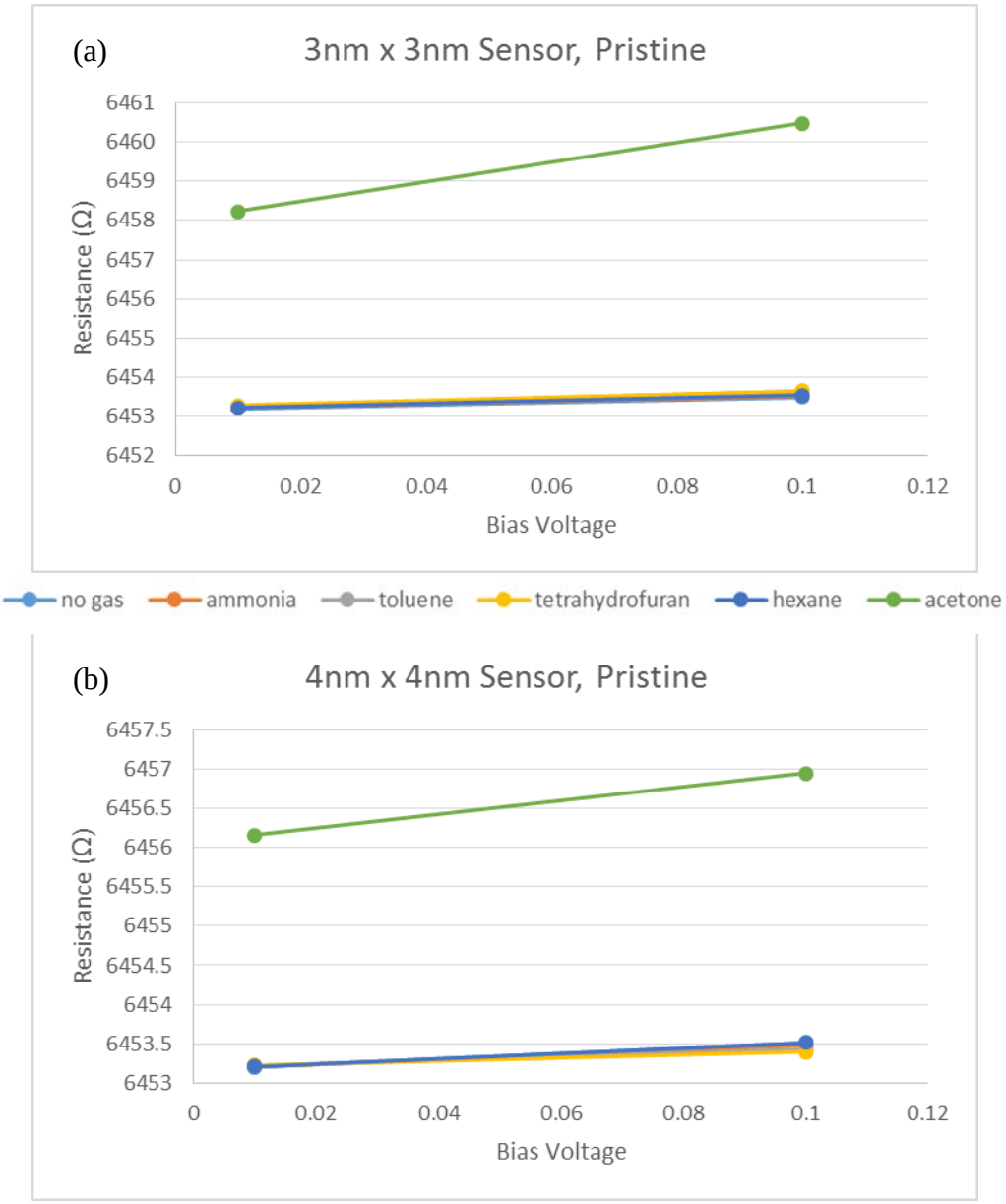

Figure 8 - Simulated resistance vs. bias voltage for a pristine graphene sensor of size (a) 3nm x 3nm and (b) 4nm x 4nm.

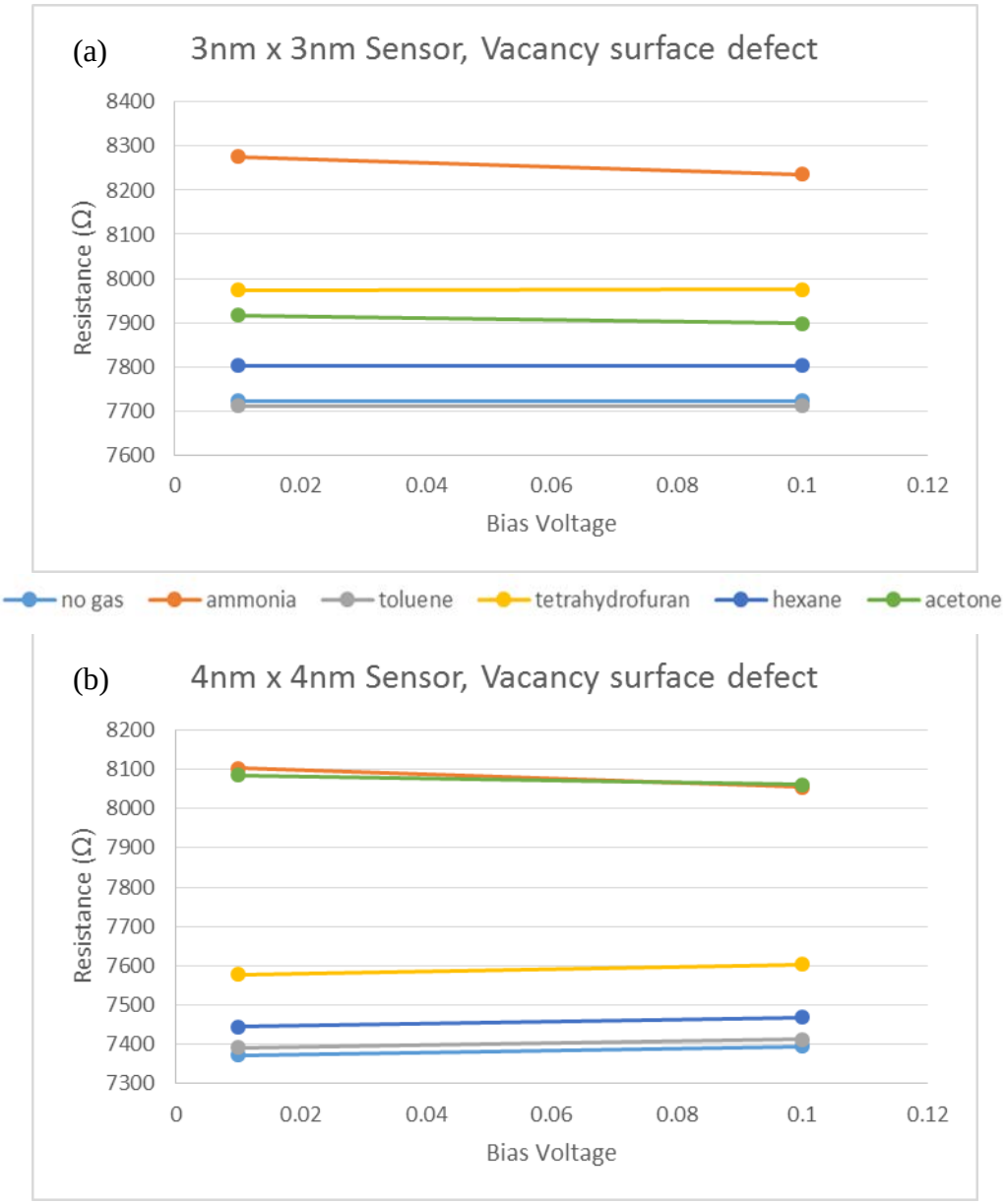

Figure 9 - Simulated resistance vs. bias voltage for a graphene sensor with a vacancy surface defect of size (a) 3nm x 3nm and (b) 4nm x 4nm.

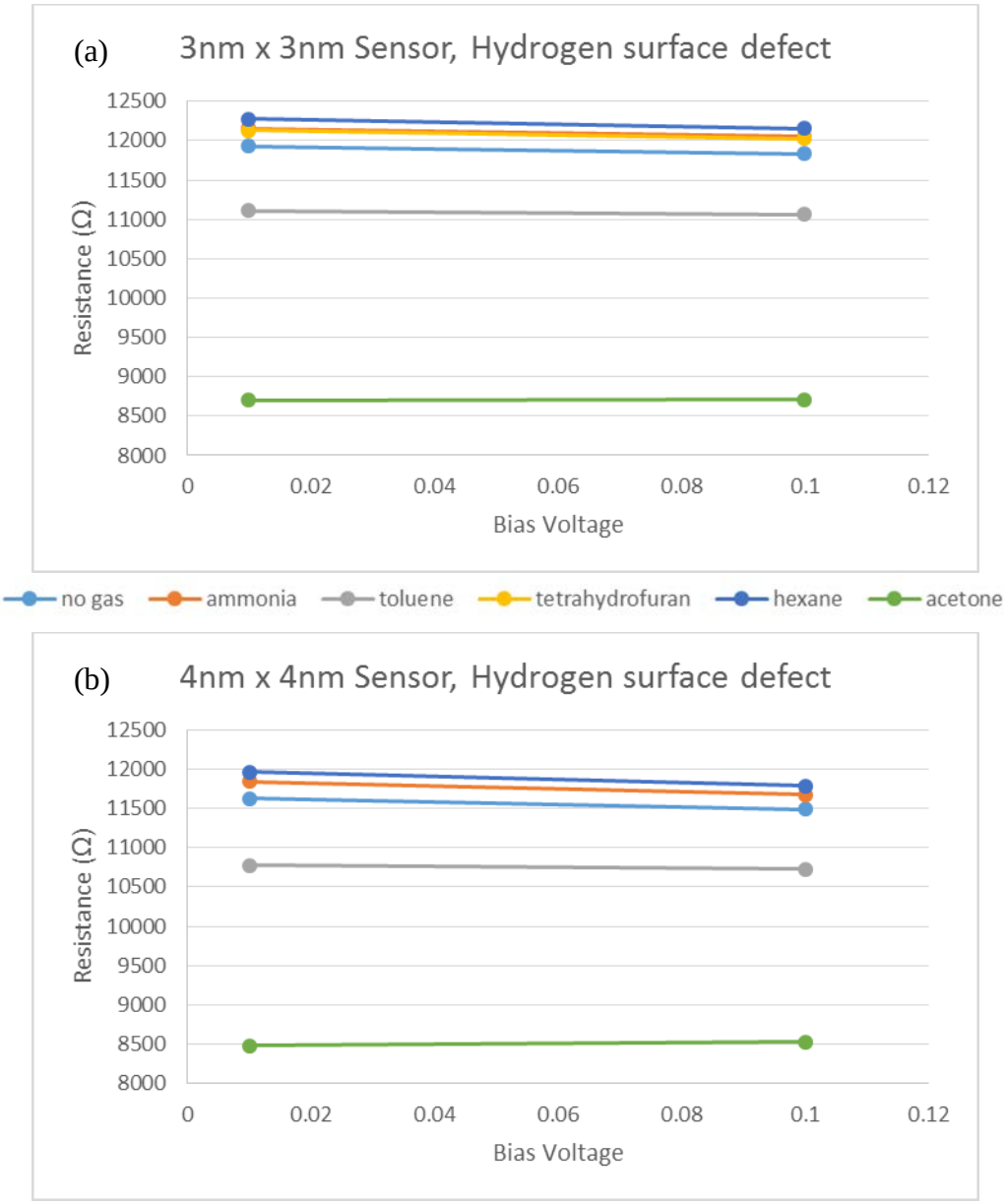

Figure 10 - Simulated resistance vs. bias voltage for a graphene sensor with a hydrogen surface defect of size (a) 3nm x 3nm and (b) 4nm x 4nm.

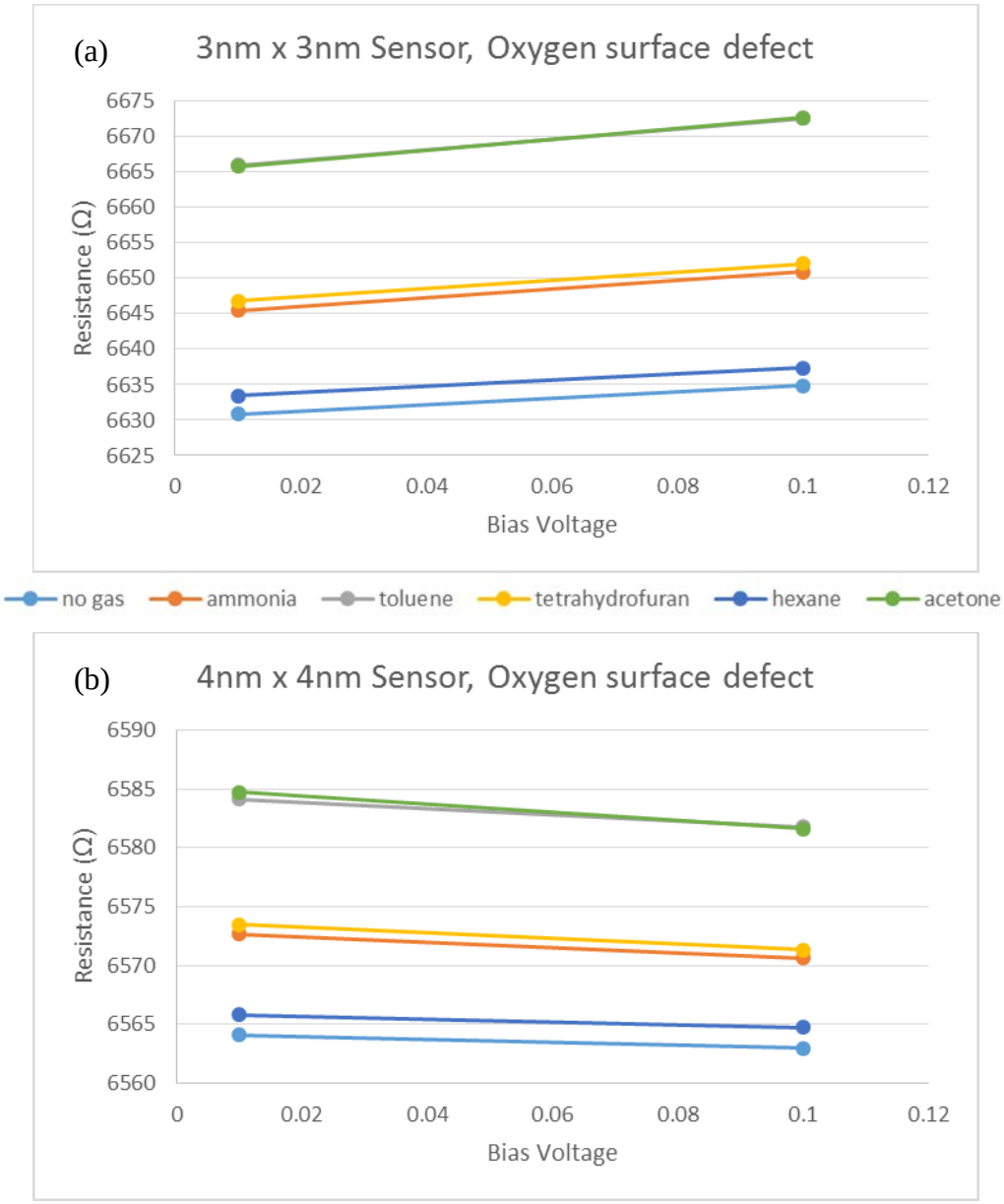

Figure 11 - Simulated resistance vs. bias voltage for a graphene sensor with an oxygen surface defect of size (a) 3nm x 3nm and (b) 4nm x 4nm.

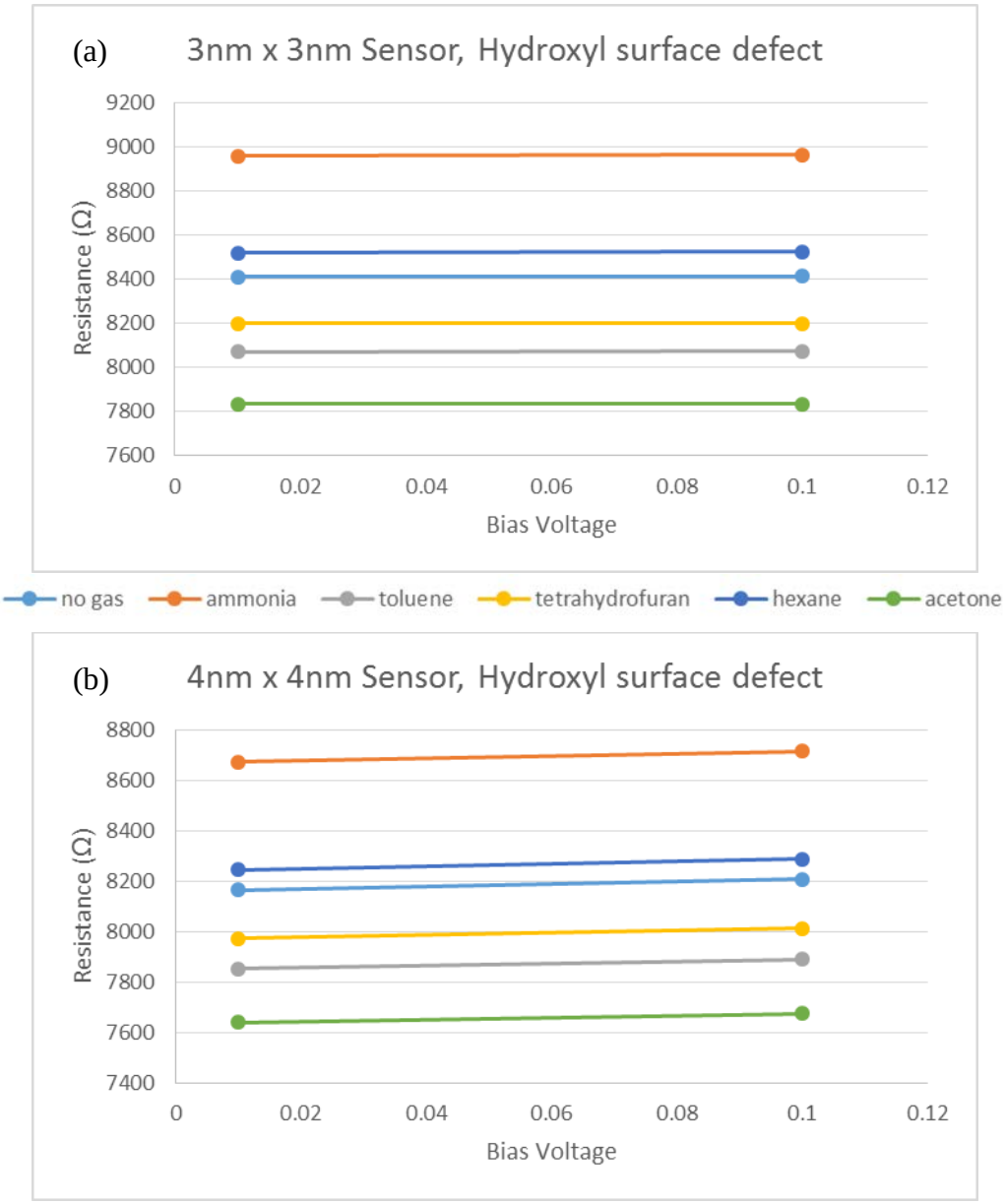

Figure 12 - Simulated resistance vs. bias voltage for a graphene sensor with a hydroxyl surface defect of size (a) 3nm x 3nm and (b) 4nm x 4nm.

Table 2 - Percentage change in resistance of a 3nm x 3nm graphene gas sensor.

Surface	V	Ammonia	Toluene	Tetrahydrofuran	Hexane	Acetone
Pristine	0.01V	0.00%	0.00%	0.00%	0.00%	0.08%
	0.1 V	0.00%	0.00%	0.00%	0.00%	0.11%
Vacancy	0.01 V	7.18%	-0.15%	3.26%	1.03%	2.51%
	0.1 V	6.67%	-0.14%	3.28%	1.04%	2.27%
Hydrogen	0.01 V	1.92%	-6.85%	1.73%	2.93%	-27.02%
	0.1 V	1.85%	-6.50%	1.63%	2.75%	-26.39%
Oxygen	0.01 V	0.22%	0.53%	0.24%	0.04%	0.53%
	0.1 V	0.24%	0.57%	0.26%	0.04%	0.57%
Hydroxide	0.01 V	6.54%	-4.02%	-2.52%	1.29%	-6.85%
	0.1 V	6.54%	-4.03%	-2.54%	1.30%	-6.88%

Table 3 - Percentage change in resistance of a 4nm x 4nm graphene gas sensor.

Surface	V	Ammonia	Toluene	Tetrahydrofuran	Hexane	Acetone
Pristine	0.01 V	0.00%	0.00%	0.00%	0.00%	0.05%
	0.1 V	0.00%	0.00%	0.00%	0.00%	0.05%
Vacancy	0.01 V	9.91%	0.26%	2.78%	0.99%	9.66%
	0.1 V	8.94%	0.24%	2.82%	1.00%	9.02%
Hydrogen	0.01 V	1.86%	-7.34%	1.57%	2.85%	-27.10%
	0.1 V	1.55%	-6.69%	1.40%	2.54%	-25.83%
Oxygen	0.01 V	0.13%	0.30%	0.14%	0.03%	0.31%
	0.1 V	0.12%	0.29%	0.13%	0.03%	0.28%
Hydroxide	0.01 V	6.20%	-3.82%	-2.35%	0.98%	-6.42%
	0.1 V	6.18%	-3.85%	-2.36%	0.98%	-6.47%

From these results, it is immediately evident that in all configurations, pristine graphene sensors show a smaller response to each gas than do sensors with any of the studied surface defects. In fact, the only gas to which a pristine graphene gas sensor appears to show any appreciable response upon exposure is acetone.

The simulations are modeled such that there is only one gas molecule being sensed when there is a gas present, and each sensor with a surface defect has only one surface defect, independent of the size of the modeled sensor. This means that the smaller sensors have a higher surface density and are sensing a higher gas concentration, both of

which were expected to lead to a larger sensor response. These results confirm this behavior as they generally show the 3nm x 3nm sensors having a larger response to the presence of a gas molecule than the 4nm x 4nm sensors. However, a larger response is seen in the larger 4nm x 4nm sensor than in the 3nm x 3nm sensor in three different situations: a sensor with a vacancy defect when exposed to ammonia, a sensor with a hydrogen defect when exposed to toluene, and a sensor with a vacancy defect when exposed to acetone. Further investigation is required to try to understand these results. One other interesting and unexpected result occurred with sensors with a vacancy defect when exposed to toluene: with the 3nm x 3nm sensor, there was a negative change in resistance; while with a 4nm x 4nm sensor, there was a positive change.

These simulation results also show that each different sensor configuration model responds differently to each different gas. That is, no sensor with the same surface configuration shows the same response to two different gases, and no two sensors with different surface configurations shows the same response to the same gas. This is an important result, as it suggests that selectively responsive sensors can be designed by decorating graphene sheets with surface defects specifically chosen to provide a desired response to a given gas while minimizing responses to other gases.

3.2 Effects of Gas Molecule Orientation

Upon initial inspection of the simulation results, it quickly became clear that there was no linear combination of surface defects that could qualitatively match the experimentally reported results for all of the gases which were chosen for performing simulations. Nallon et al. reported that their graphene gas sensor showed a negative

change in resistance when exposed to hexane. However, the simulations showed a positive change in resistance for all sensor surface configurations.

Leenaerts et al. reported that the orientation of a gas molecule above a graphene surface has a strong effect on charge transfer and adsorption energy.[13] In light of these findings, simulations were performed with some of the molecules in a different orientation above a graphene surface defect to determine what effect it would have on the results. The hydrogen surface defect sensor configuration was chosen to investigate the effect of molecule orientation. This surface defect was chosen because there was an anomalously large change in resistance when exposed to acetone (approximately -27% as compared to $<\pm 10\%$ for every other surface defect and gas molecule combination), and it was hypothesized that this could be accounted for by an incorrect orientation of the acetone molecule. The acetone molecule was rotated by approximately 90°, which is referred to as orientation 2 (with orientation 1 referring to the original orientation of the molecule in the simulations). A relaxation was then performed on the new geometry. Figure 12 shows both orientation 1 and orientation 2 of the acetone molecule with respect to the graphene gas sensor. The I-V curve simulation was re-run, and the new percent change in resistance was drastically different than the result achieved with the acetone molecule in orientation 1. Table 4 lists the percent change in resistance for a graphene sensor with a hydrogen defect in the presence of acetone in both orientation 1 and orientation 2. With the acetone molecule in orientation 1, the simulations resulted in a percent change in resistance of approximately -27%. However, with the acetone molecule in orientation 2, the simulations showed a percent change of approximately 1.4%. This

makes the importance of molecule orientation starkly clear, as the change in orientation of the acetone molecule resulted not only a drastic change in magnitude of the change in resistance, but also a change in sign.

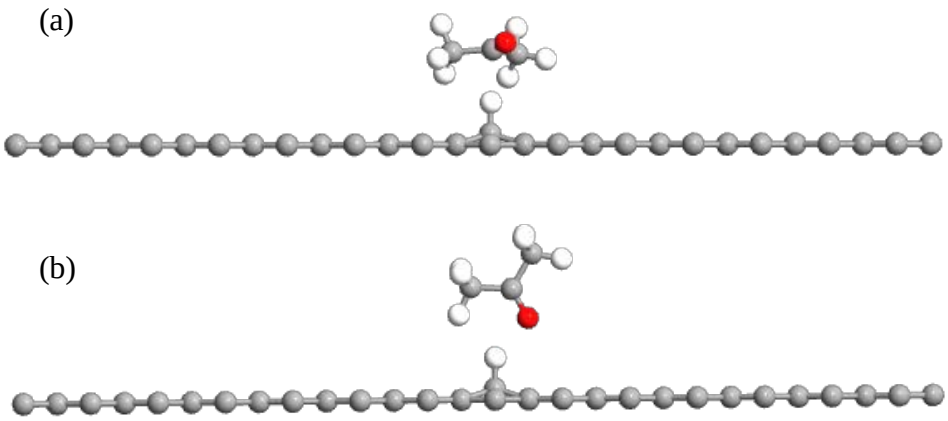

Figure 13 - (a) Orientation 1 of acetone molecule (b) Orientation 2 of acetone molecule

With this new orientation of acetone, the graphene sensor with a hydrogen trap had the correct sign for change in resistance when exposed to all gases except for hexane. In light of the discovery that a change in the orientation of the sensed molecule could lead to altering the sign of the change in resistance, the orientation of the hexane molecule was also changed. The hexane molecule was rotated by approximately 90° which is again referred to as orientation 2, as opposed to orientation 1 for the original orientation. A relaxation was performed on the new geometry. Figure 13 shows both orientation 1 and orientation 2 of the hexane molecule with respect to the graphene gas sensor. The I-V curve simulation was re-run, and the new percent change was determined. Table 4 lists the percent change in resistance for a graphene sensor with a hydrogen defect in the

presence of hexane in both orientation 1 and orientation 2. With the acetone molecule in orientation 1, the simulations resulted in a positive percent change in resistance, while in orientation 2, the simulations showed a negative change in resistance.

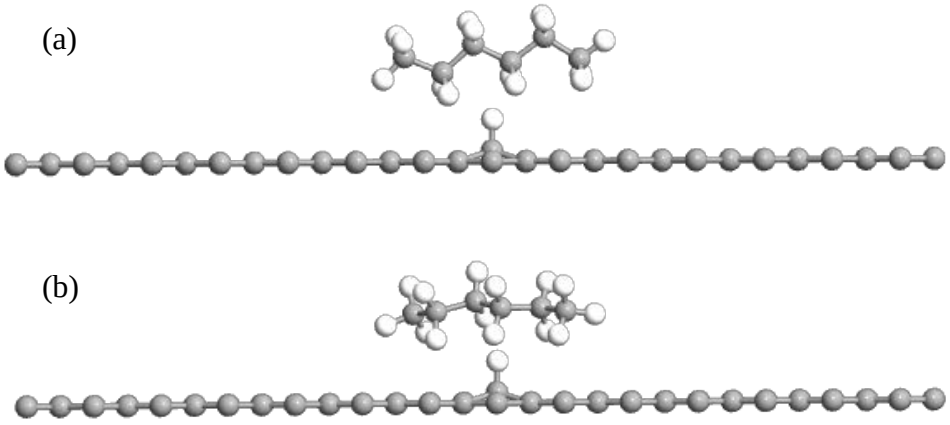

Figure 14 - (a) Orientation 1 of hexane molecule (b) Orientation 2 of hexane molecule

Table 4 - Percentage change in resistance for a graphene sensor with a hydrogen surface defect due to different orientations of a gas molecule.

Gas	V	3nm x 3nm orientation 1	3nm x 3nm orientation 2	4nm x 4nm orientation 1	4nm x 4nm orientation 2
Acetone	0.01 V	-27.0%	1.41%	-27.1%	1.38%
	0.1 V	-26.4%	1.39%	-25.8%	1.12%
Hexane	0.01 V	2.93%	-2.37%	2.85%	-2.33%
	0.1 V	2.75%	-2.24%	2.54%	-2.11%

3.3 Comparison of Computed and Experimental Results

As noted above, with all of the molecules in the originally modeled orientation (orientation 1), the simulation results showed no sensor configuration that gave a negative change in resistance for hexane, and therefore no linear combination of surface defects could match all of the experimentally reported results. Replacing the results for the hydrogen surface defect sensing acetone and hexane in orientation 1 with the results

with acetone and hexane in orientation 2 alters this situation. Including those results, the graphene sensor with a hydrogen surface defect shows a positive change in resistance for ammonia, tetrahydrofuran, and acetone, and a negative change in resistance for toluene and hexane. This matches the experimental results reported by Schedin et al. and Nallon et al. for these molecules. Accordingly, it appears that the sensors used in these experiments showed sensing behavior dominated by hydrogen surface defects.

3.4 Quasi-Dynamic Sensor Behavior Modeling

Figures 15-20 show the results of simulations of the dynamic response of a graphene gas sensor. For these simulations, a graphene gas sensor with a hydrogen surface defect was used, due to the fact that the simulated response of this surface configuration appeared to match experimental responses found in the literature. Each chart in Figures 15-20 shows the response of a graphene gas sensor with a hydrogen surface defect when exposed to one of the 5 studied gases: acetone, ammonia, tetrahydrofuran, hexane, and toluene. Each of these charts shows the percent change in resistance from a baseline in which no gas is present, including the situation when no gas molecule is present and when a sensed gas molecule is placed 3Å higher than the optimized height, 2Å higher than the optimized height, 1Å higher than the optimized height, and at the optimized height.

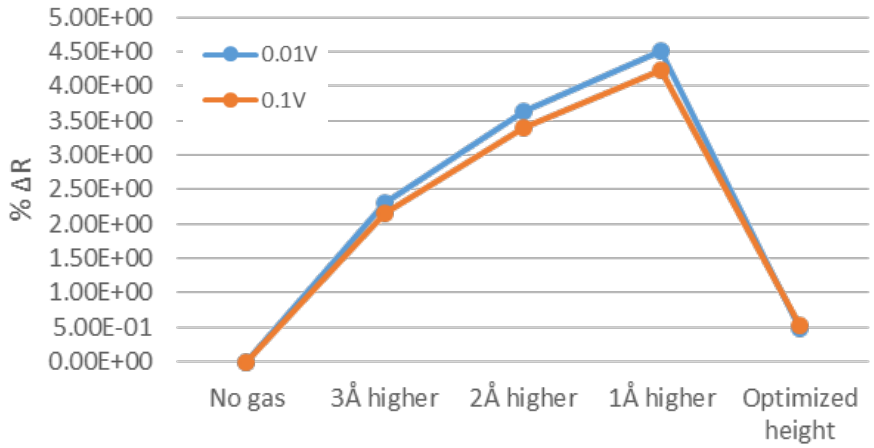

Figure 15 - Quasi-dynamic simulation results for acetone.

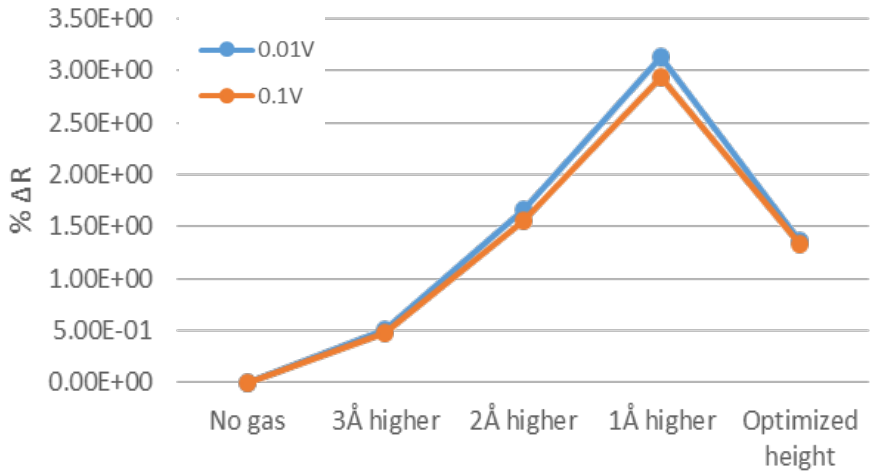

Figure 16 - Quasi-dynamic simulation results for ammonia.

Figures 15 and 16 show the results for simulations with acetone and ammonia, respectively. The simulated sensor shows an increase in %ΔR for both acetone and ammonia as the gas molecule approaches the sensor (modeled average distance gets smaller), up until the sensed molecule reaches a modeled average distance of 1Å. However, when the molecule is located at the optimized height (modeled average distance of 0Å), the sensor shows a decrease in %ΔR. It is hypothesized that this decrease

in response at the optimized height is due to the fact that the optimized height is a low energy position.

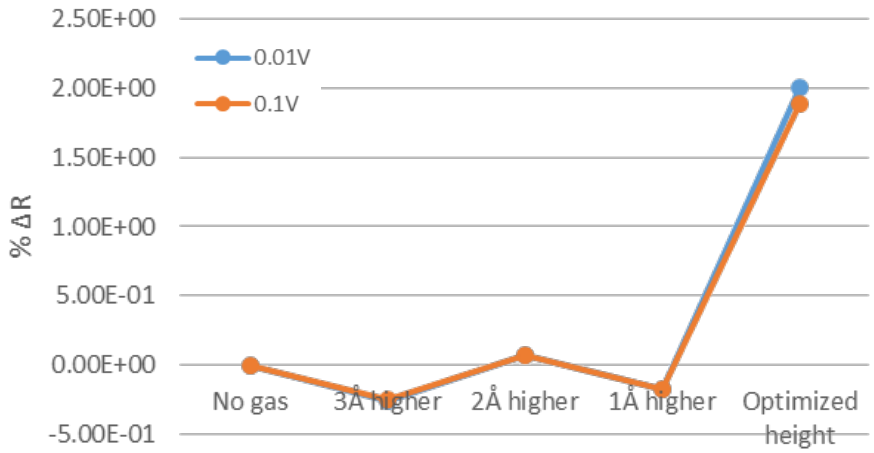

Figure 17 - Quasi-dynamic simulation results for tetrahydrofuran.

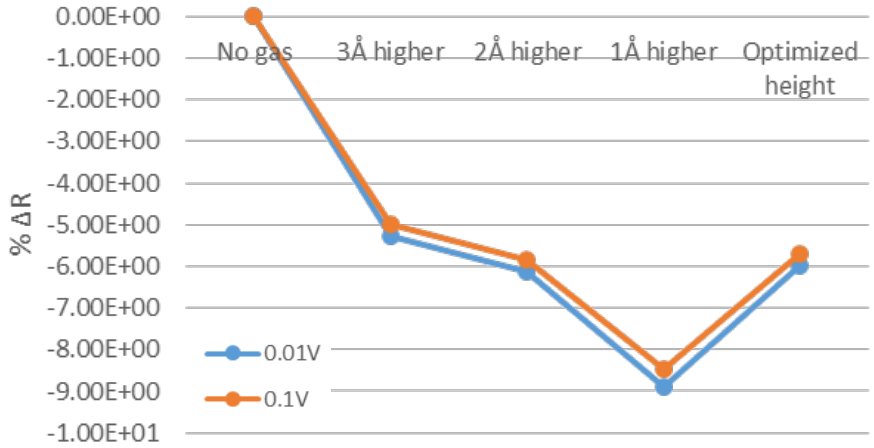

Figure 18 - Quasi-dynamic simulation results for toluene.

Figures 17 and 18 show the results for simulations with tetrahydrofuran and toluene, respectively. The simulated sensor shows almost no change in %ΔR upon exposure to tetrahydrofuran as the molecule approaches the sensor (modeled average distance gets smaller), up until the sensed molecule reaches a modeled average distance of 1Å. When the molecule reaches the optimized height (modeled average distance of

0Å), the sensor shows an increase in %ΔR. The simulated sensor response to toluene is similar to the response shown in Figures 15 and 16 for ammonia and acetone, except that the %ΔR shows a different sign. Thus, the simulated sensor shows a decrease in %ΔR for toluene as the gas molecule approaches the sensor (modeled average distance gets smaller), up until the sensed molecule reaches a modeled average distance of 1Å. When the molecule is located at the optimized height (modeled average distance of 0Å), the sensor shows an increase in %ΔR. Again, it is hypothesized that this decrease in response magnitude at the optimized height is due to the fact that the optimized height is a low energy position.

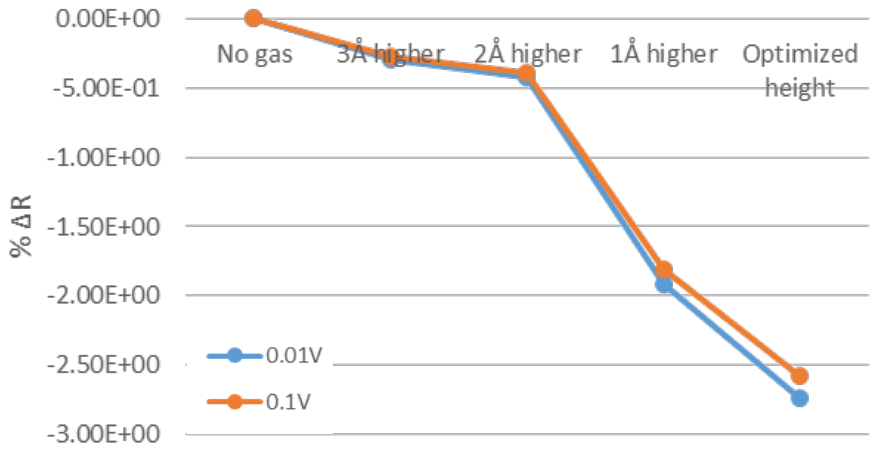

Figure 19 - Quasi-dynamic simulation results for hexane.

Figure 19 shows the results for simulations with hexane. Of the five gases that were simulated, only hexane shows a monotonic response across all modeled average distances. The simulated sensor shows a decrease in %ΔR for hexane as the gas molecule approaches the sensor (modeled average distance gets smaller) all the way down to the optimized height (modeled average distance of 0Å).

The quasi-dynamic simulation data was then used to try to match the curves reported by Nallon et al.[17] A curve fit was only attempted with the hexane data shown in Figure 19 because this data was monotonic. The collected data was fit to a curve of the form $\%\Delta R = A(1-e^{kt})$ which was adjusted to show a time scale similar to the time scales of the responses reported by Nallon et al.[17] Figure 20 shows the result of this curve fit, and Figure 21 shows the curves reported by Nallon et al.[17] A visual comparison of the two graphs shows a reasonable match between the shape of the simulated data and the experimentally reported data.

Figure 22 shows the data of Figure 20 replotted as modeled average distance vs. time rather than $\%\Delta R$ vs. time. This chart shows that modeled average distance is an unrealistic model of the behavior of an actual individual molecule as the chart shows a time of approximately 20 seconds for modeled average distance to reach 0Å (optimized height). This would be a surprisingly long amount of time for a single molecule to reach its final equilibrium state. However, the close match between Figures 20 and 21 shows that modeled average distance may be a useful parameter when modeling the dynamics of an entire sensing system.

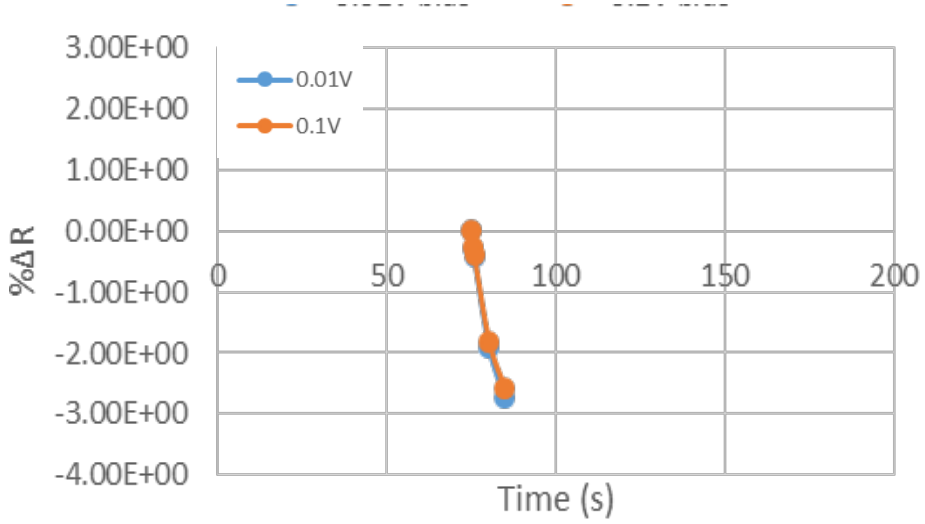

Figure 20 - Curve fit of simulated quasi-dynamic data to a curve of the form $\%\Delta R = A(1-e^{kt})$ on the same time scale as the data reported by Nallon et al.

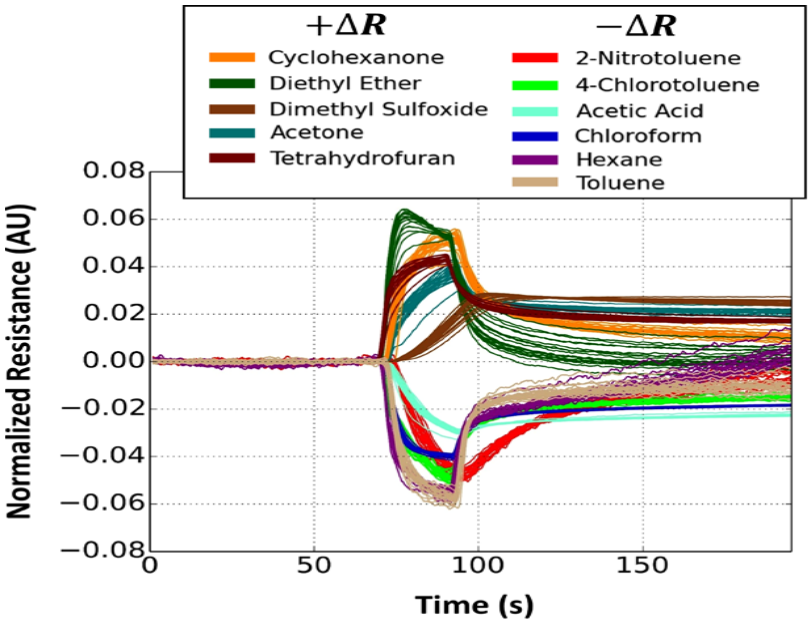

Figure 21 - Experimental graphene sensor response data reported by Nallon et al.[17]

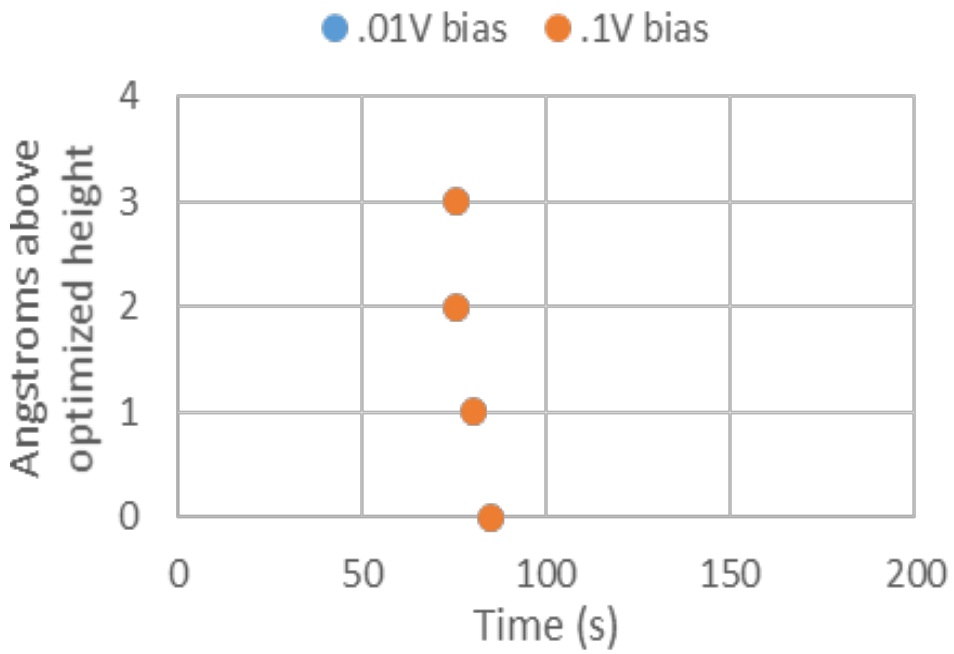

Figure 22 - Curve fit of simulated quasi-dynamic data to a curve of the form $\%\Delta R = A(1-e^{kt})$ plotted as Angstroms above optimized height (modeled average distance) vs. time.

CHAPTER 4 – SUMMARY AND FUTURE RESEARCH

4.1 Summary

The key role that surface defects play in the sensing behavior of graphene gas sensors was demonstrated using first-principles simulation of graphene gas sensors with different surface defects in the presence of ammonia, toluene, tetrahydrofuran, hexane, and acetone. Pristine graphene sensors showed minimal response to gases, whereas sensors with surface defects showed significantly greater sensitivity. Sensors with different surface configurations responded differently to the same gases, indicating that it is possible to engineer sensors to provide a specific and selective response to gases. It was demonstrated that molecule orientation with respect to the graphene sensor surface has a significant impact on sensing behavior. Based on a comparison between the simulated data and experimentally reported data, it was determined that the response of graphene gas sensors used by Schedin et al. and Nallon et al. were likely dominated by hydrogen surface defects. Quasi-dynamic simulations were performed to investigate the dynamics of sensing behavior. These simulations were able to reasonably model experimental response to at least some gasses, though the simulations are not a reliable model of individual gas molecule behavior.

4.2 Future Research

The results obtained from the research presented herein suggest many interesting directions for further research. Investigation into the effects of molecule orientation with respect to the graphene sensor should be expanded to include all of the studied molecules and all of the studied surface defect configuration. Careful analysis should be performed to determine the lowest energy orientation for each molecule/surface defect combination. Furthermore, simulations including different surface defects and functionalizations should be performed in order to gain more information as to how to tailor graphene sensors to provide desired responses. Surface functionalization with nickel, carboxylic acid, and simple polymers could all be explored through well-designed first-principles simulations. Yet another important direction for further research is an investigation of how a combination of surface defects would affect sensor response. All of the results presented in this work were obtained from simulations of sensors with only a single surface defect. Simulations showing the response of sensors with multiple surface defects of different types would provide further knowledge on how to design graphene sensors that would provide a desired response to specific molecules.

REFERENCES

1. Global Sensor Market 2016, Allied Market Research (AMR), (2016).

2. Chemical Sensors Market Trends, Global Industry Analysts, Inc., (2015).

3. G. Chansin and D. Pugh, Environmental Gas Sensors 2017-2027, IDTechEx, (2017).

4. B. Szulczynski and J. Gebicki. “Currently Commercially Available Chemical Sensors Employed for Detection of Volatile Organic Compounds in Outdoor and Indoor Air.” Environments, 2017, 4, 21.

5. A. Nayyar, V. Puri, and D.-N. Le. “A Comprehensive Review of Semiconductor-Type Gas Sensors for Environmental Monitoring.” Review of Computer Engineering Research, 2016, 3(3): 55-64.

6. W. P. Jakubik. “Surface Acoustic Wave-Based Gas Sensors.” Thin Solid Films, 520 (2011) 986-993.

7. H. Xie, Q. Yang, X. Sun, J. Yang, and Y. Huang. “Gas Sensor Arrays Based on Polymer-Carbon Black to Detect Organic Vapors at Low Concentration.” Sensors and Actuators B: Chemical, 113 (2006) 887-891.

8. J. R. Li, J. R. Xu, M. Q. Zhang, and M. Z. Rong. “Carbon Black/Polystyrene Composites as Candidates for Gas Sensing Materials.” Carbon, 41, (2003) 2353-2360.

9. J. Li, Y. Lu, Q. Ye, M. Cinke, J. Han, and M. Meyyappan. “Carbon Nanotube Sensors for Gas and Organic Vapor Detection.” Nano Letters, 2003, 3 (7) 929-933.

10. J. Kong, N. R. Franklin, C. Zhou, M. G. Chapline, S. Peng, K. Cho, and H. Dai. “Nanotube Molecular Wires as Chemical Sensors.” Science, 287, (2000) 622-625.

11. E. C. Nallon, “Graphene-Based Chemical Vapor Sensors for Electronic Nose Applications.” Ph.D. Dissertation, George Mason University, 154pp, (2016).

12. K. R. Amin and A. Bid. “Graphene as a Sensor.” Current Science, 2014, 107, 3 430-436.

13. F. Schedin, A. K. Geim, S. V. Morozov, E. W. Hill, P. Blake, M. I. Katsnelson, and K. S. Novoselov. “Detection of Individual Gas Molecules Adsorbed on Graphene”. Nature Materials, 2007, 6, 652–655.

14. O. Leenaerts, B. Partoens, and F. M. Peeters. “Adsorption of H_2O, NH_3, CO, NO_2, and NO on Graphene: A First-Principles Study.” Physical Review B. **77**, 124516 (2008).

15. G. Ko, H.-Y. Kim, J. Ahn, Y.-M. Park, K.-Y. Lee, and J. Kim. “Graphene-Based Nitrogen Dioxide Gas Sensors.” Current Applied Physics 10 (2010) 1002-1004.

16. G. Chen, T. M. Paronyan, and A. R. Harutyunyan. “Sub-ppt Gas Detection with Pristine Graphene.” Applied Physics Letters, 101, 053119 (2012).

17. E. C. Nallon, V. P. Schnee, C. Bright, M. P. Polcha, and Q. Li. “Chemical Discrimination with an Unmodified Graphene Chemical Sensor.” ACS Sensors 2016, 1, 26-31.

18. Y. Seekaew, D. Phokharatkul, A. Wisitsoraat, and C. Wongchoosuk. “Highly Sensitive and Selective Room-Temperature NO2 Gas Sensor Based on Bilayer Transferred Chemical Vapor Deposited Graphene.” Applied Surface Science, 404 (2017) 357-363.

19. F. Schwierz. “Graphene Transistors.” Nature Nanotechnology, 2010, 5, 487-496.

20. J. A. Robinson, E. S. Snow, S. C. Badescu, T. L. Reinecke, and F. K. Perkins. “Role of Defects in Single-Walled Carbon Nanotube Chemical Sensors.” Nano Letters, 2006, 6 (8) 1747-1751.

21. A. Saleh-Khojin, D. Estrada, K. Y. Lin, M. Bae, F. Xiong, E. Pop, and R. I. Masel. “Polycrystalline Graphene Ribbons as Chemiresistors.” Advanced Materials, 2012, 24, 53-57.

22. Y. Dan, Y. Le, N. J. Kybert, Z. Luo, and A. T. C. Johnson. “Intrinsic Response of Graphene Vapor Sensors.” Nano Letters, 2009, 9 (4) 1472-1475.

23. X. L. Wei, Y. P. Chen, W. L. Liu, and J. X. Zhong. “Enhanced Gas Sensor Based on Nitrogen-Vacancy Graphene Nanoribbons.” Physics Letters A, 376 (2012) 559-562.

24. Y. H. Zhang, Y. B. Chen, K. G. Zhou, C. H. Liu, J. Zeng, H. L. Zhang, and Y. Peng. "Improving Gas Sensing Properties of Graphene by Introducing Dopants and Defects: A First-Principles Study." *Nanotechnology*, 20 (2009) 185504.

25. X. Y. Lieu, J. M. Zhang, K. W. Xu, and V. Ji. "Improving SO2 Gas Sensing Properties of Graphene by Introducing Dopant and Defect: A First-Principles Study." Applied Surface Science, 313¸ (2014) 405-410.

26. D. Yang, N. Yang, J. Ni, J. Xiao, J. Jiang, Q. Liang, T. Ren, and X. Chen. "First-Principles Approach to Design and Evaluation of Graphene as Methane Sensors." Materials and Design, 119 (2017) 397-405.

27. QuantumWise, QunatumWise (online). Available: http://www.quantumwise. com/ [accessed 22.06.17]

28. H. Raza and E.C. Kan. "An Extended Huckel Theory Based Atomistic Model for Graphene Nanoelectronics." Journal of Computational Electronics, (2008) 7: 372-375.

BIOGRAPHY

Aaron Lowenberger graduated from Delsea Regional High School in Franklin Township, NJ, in 1998. He received his Bachelor of Science degree in Electrical Engineering from Boston University in 2002. He has worked as a Patent Examiner at the United States Patent and Trademark Office since 2011.